Reciprocity Relations in Waveguide Junctions

Dylan F. Williams and Roger B. Marks

Abstract— **The Lorentz reciprocity condition is applied to junctions composed of reciprocal media which connect uniform but otherwise arbitrary waveguides. An expression relating the forward and reverse transmission coefficients is derived and factored into two terms: the first involving the phase of the reference impedance in the guide, and the second a new reciprocity factor. The usual condition equating the forward and reverse transmission coefficients is shown not to hold in the general case. Experimental evidence supporting the theoretical results is presented.**

I. Introduction

In this work we consider the conditions relating the scattering parameters of reciprocal waveguide junctions, that is, junctions containing only linear materials with symmetric permittivity and permeability tensors. The junctions are assumed to be connected to uniform waveguides in which only a single mode of propagation is significantly excited.

If the waveguides are lossless, the forward and reverse transmission coefficients of a reciprocal junction may be equated as a result of the Lorentz reciprocity theorem [1]. This well-known condition is especially useful when only the product of the forward and reverse transmission coefficients can be directly measured, as is the case in certain de-embedding algorithms [2].

With the increasing use of planar transmission lines and integrated circuits, junctions between waveguides supporting lossy hybrid modes have become common. Microwave wafer probes, which interconnect coaxial and coplanar lines, typify such junctions. In these instances, the usual microwave circuit theories (e.g., [1]) fail. This opens the possibility that the forward and reverse transmission coefficients of the junction may be unequal.

This work applies the Lorentz reciprocity theorem to determine the relationship between the forward and reverse transmission coefficients of an arbitrary reciprocal junction. The derivation is based upon a general circuit theory [3] which applies to lossy hybrid modes such as those found in coplanar waveguide (CPW) or microstrip lines. The relationship is shown to involve two terms: one dependent on the phase angle of the reference impedance in the guide, and the other on a new term, which we call the reciprocity factor. For illustration, we calculate these terms for several guides. We also present experimental measurements, which are consistent with the theory, of the ratio of the forward and reverse transmission coefficients of a microwave probe. Some of these results have been presented in [4].

Manuscript received May 3, 1991; revised November 30, 1992. This work was supported by the NIST Director's Reserve.

The authors are with the National Institute of Standards and Technology, Boulder, CO 80303.

IEEE Log Number 9209335.

II. Scattering Parameters

Scattering parameters, which include the transmission coefficients of interest here, are conventionally defined to relate the waves in the various waveguides attached to a junction. However, many definitions of these waves are in common use. Here we take a very general approach, making use of the pseudowaves defined in [3]. These quantities are defined much like ordinary traveling waves, which depend exponentially on the axial coordinate. However, the definition makes use of an arbitrary reference impedance. When this reference impedance is equal to the characteristic impedance of the waveguide, the pseudowaves reduce to the traveling waves. Otherwise, the pseudowaves are simply traveling waves that have been subjected to an impedance transform. This definition accommodates practical situations that demand the use of a particular reference impedance. Commercial microwave design tools restricted to the use of real reference impedances provide one example. The definition is also closely connected to the measurement process, in which the reference impedance is determined by the calibration rather than simply defined in an abstract sense.

Consider a two-port junction connected to two dissimilar uniform semiinfinite waveguides. In each waveguide, a reference plane is chosen far enough from the junction that higher-order modes are insignificant. Following the general treatment of [3], which includes lossy lines, the characteristic impedance of the mode may be defined from the modal transverse electric field $\boldsymbol{e}_n$ and magnetic field $\boldsymbol{h}_n$ of the forward propagating mode by

$$Z_{on} \equiv \frac{|\nu_{on}|^2}{p_{on}^*}, \tag{1}$$

where

$$p_{on} \equiv \int_{\sigma_n} \boldsymbol{e}_n \times \boldsymbol{h}_n^* \cdot \hat{\boldsymbol{n}}\, dS \tag{2}$$

is the complex power carried across the surface σ_n, coincident with the reference plane in the nth guide (see Fig. 1), by the normalized forward mode. The constant v_{on} is defined by

$$\nu_{on} \equiv -\int_{\text{path}} \boldsymbol{e}_n \cdot d\boldsymbol{l}, \tag{3}$$

and $\hat{\boldsymbol{n}}$ is the unit vector normal to σ_n directed into the junction. The integration path in (3) lies in σ_n and a time dependence $e^{j\omega t}$ is assumed. The phase of Z_{on} is independent

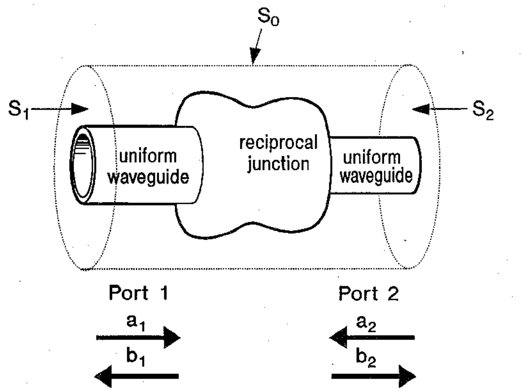

Fig. 1. A general two-port junction. The surfaces σ_1 and σ_2 are coincident with the two waveguide ports of the junction. The surface σ_0 in this case is a cylinder, which may extend to infinity. The surface $\sigma_0 + \sigma_1 + \sigma_2$ encloses the entire junction.

of the normalization imposed by the choice of integration path. Although Z_{on} is real in lossless lines, it is, in general, complex.

We next define the waveguide voltage v_n and current i_n in terms of the total transverse electric and magnetic fields $\boldsymbol{E}_{in}$ and $\boldsymbol{H}_{in}$ in the guide

$$\boldsymbol{E}_{tn} = \frac{v_n}{v_{on}} \boldsymbol{e}_n; \qquad \boldsymbol{H}_{tn} = \frac{i_n}{i_{on}} \boldsymbol{h}_n \tag{4}$$

where $i_{on} \equiv v_{on}/Z_{on}$.

We then define the pseudowave amplitudes [3] as linear combinations of v_n and i_n:

$$a_n(Z_{rn}) = \frac{|v_{on}|}{v_{on}} \frac{\sqrt{\mathrm{Re}(Z_{rn})}}{2|Z_{rn}|}(v_n + i_n Z_{rn}) \tag{5}$$

and

$$b_n(Z_{rn}) = \frac{|v_{on}|}{v_{on}} \frac{\sqrt{\mathrm{Re}(Z_{rn})}}{2|Z_{rn}|}(v_n - i_n Z_{rn}). \tag{6}$$

Each waveguide's reference impedance Z_{rn} is arbitrary except for restriction $\mathrm{Re}(Z_{rn}) > 0$ [3]. The normalization used in (5) and (6) is chosen to meet three criteria. The magnitude enforces a power normalization of the pseudowaves. The phase simplifies the reciprocity relations determined below. And, finally, when Z_{rn} is chosen to equal Z_{on}, the pseduowaves reduce to the traveling waves, which depend exponentially on the axial coordinate.

The net flow of power across the nth port may be written in terms of the pseudowave amplitudes as

$$P_n \equiv \mathrm{Re} \int_{\sigma_n} \boldsymbol{E}_{tn} \times \boldsymbol{H}_{tn}^* \cdot \hat{\boldsymbol{n}}\, dS = \mathrm{Re}(v_n i_n^*) = |a_n|^2 - |b_n|^2 + 2\,\mathrm{Im}(a_n b_n^*) \frac{\mathrm{Im}(Z_{rn})}{\mathrm{Re}(Z_{rn})}. \tag{7}$$

Notice that, because of the cross term $a_n b_n^*$, the power is not simply the difference of the powers that would be carried by the forward and backward pseudowaves acting alone. The cross term, however, vanishes when Z_{rn} is real

The pseudoscattering parameters S_{nm} of a junction are defined in terms of the pseudowave amplitudes at each port in the conventional way as

$$b_m = \sum_n S_{mn} a_n \tag{8}$$

where the sum extends over all of the ports. Although not denoted explicitly in (8), the pseudoscattering parameters are functions of the reference impedances Z_{rn}. For the special case when $Z_{rn} = Z_{on}$ at each port, the pseudoscattering parameters reduce to the conventional S-parameters, defined by

$$b_m(Z_{om}) = \sum_n S_{mn}^o a_n(Z_{on}). \tag{9}$$

Because the traveling waves $a_n(Z_{on})$ and $b_n(Z_{on})$ are the physical waves that propagate in the line, the S_{mn}^o are directly measurable with slotted line techniques or with a vector network analyzer calibrated with the thru-reflect-line (TRL) technique [3]. The pseudowave S-parameters of (8) are simply an impedance-transformed form of the S_{mn}^o.

The pseudowaves defined by (5) and (6) should not be confused with the power waves defined by Kurokawa [5]. The power waves are not related to the traveling waves by an impedance transform [3]. They also do not correspond to the S-parameters determined by any conventional network analyzer calibration method.

III. Reciprocal Junctions

The fields at each port of a waveguide junction may be written as a superposition of the modal electric and magnetic fields. For a two-port junction, it is always possible to find sources J_1 and J_2 placed outside the junction so that

$$\hat{\boldsymbol{n}} \times \boldsymbol{E}_t(J_1)\big|_{\sigma_2} = 0 \tag{10}$$

and

$$\hat{\boldsymbol{n}} \times \boldsymbol{E}_t(J_2)\big|_{\sigma_1} = 0 \tag{11}$$

where $\boldsymbol{E}_t(J_n)$ is the field due to sources J_n. Now, (10) and (11) are equivalent to

$$a_2(J_1) + b_2(J_1) = a_1(J_2) + b_1(J_2) = 0 \tag{12}$$

where the arguments J_n again indicate the source. If the junction is reciprocal, the Lorentz reciprocity condition [1] gives

$$\oint_{\sigma_1+\sigma_2+\sigma_0} (\boldsymbol{E}_t(J_1) \times \boldsymbol{H}_t(J_2) - \boldsymbol{E}_t(J_2) \times \boldsymbol{H}_t(J_1)) \cdot \hat{\boldsymbol{n}}\, dS = 0 \tag{13}$$

where the surface $\sigma_1 + \sigma_2 + \sigma_0$ encloses the entire junction, as shown in Fig. 1, and $\hat{n}$ is the unit normal pointing into the junction. If the fields are zero on σ_0, or if σ_0 is a perfectly conducting surface, is characterized by a scalar surface impedance, or is infinitely far away, the integral vanishes there [1]. Conditions (10) and (11) may be further used to simplify (13), which reduces to

$$\int_{\sigma_1} \boldsymbol{E}_t(J_1) \times \boldsymbol{H}_t(J_2) \cdot \hat{\boldsymbol{n}}\, dS = \int_{\sigma_2} \boldsymbol{E}_t(J_2) \times \boldsymbol{H}_t(J_1) \cdot \hat{\boldsymbol{n}}\, dS. \tag{14}$$

Using (4), (5), and (6), $\boldsymbol{E}_t$ and $\boldsymbol{H}_t$ may be expressed in terms of the pseudowave amplitudes. Using these expressons in (14) results in

$$[a_1(J_1)+b_1(J_1)][a_1(J_2)-b_1(J_2)]K_1\frac{Z_{r1}^*}{\mathrm{Re}(Z_{r1})} = [a_2(J_2)+b_2(J_2)][a_2(J_1)-b_2(J_1)]K_2\frac{Z_{r2}^*}{\mathrm{Re}(Z_{r2})} \quad (15)$$

where the reciprocity factor K_n is defined as

$$K_n \equiv \frac{Z_{on}}{|v_{on}|^2}\int_{\sigma_n} \boldsymbol{e}_n\times\boldsymbol{h}_n\cdot\hat{\boldsymbol{n}}\,dS = \frac{\overline{p}_{on}}{p_{on}^*}. \quad (16)$$

Here

$$\overline{p}_{on} \equiv \int_{\sigma_n} \boldsymbol{e}_n\times\boldsymbol{h}_n\cdot\hat{\boldsymbol{n}}\,dS. \quad (17)$$

While (15) relates the pseudowave amplitudes at the two ports only for the sources J_1 and J_2, it actually forces some conditions on the S-parameters, as we will now show. First, the b_n of (15) can be replaced by expressions involving only the a_n and the S-parameters using (8) and (12) with the result

$$a_1(J_2)[a_1(J_1)(1+S_{11})+S_{12}a_2(J_1)]K_1\frac{Z_{r1}^*}{\mathrm{Re}(Z_{r1})} = a_2(J_1)[a_2(J_2)(1+S_{22})+S_{21}a_1(J_2)]K_2\frac{Z_{r2}^*}{\mathrm{Re}(Z_{r2})} \quad (18)$$

Next, the reflection coefficients can be eliminated from the bracketed expressions in (18) with the relations $(1+S_{mm}) = -S_{mn}a_n(J_n)/a_m(J_n)$ for $n \neq m$ derived from (8) and (12). The transmission parameters factor out of the resultant expressions leaving identical terms involving the a_n on both sides of the equation. This results in an expression that relates only the transmission parameters

$$S_{12}K_1\frac{Z_{r1}^*}{\mathrm{Re}(Z_{r1})} = S_{21}K_2\frac{Z_{r2}^*}{\mathrm{Re}(Z_{r2})}. \quad (19)$$

Equation (19) is easily extended to multiport junctions by terminating all but the mth and nth ports in perfect matches, and including those terminations within the surface σ_0. The result is

$$\frac{S_{nm}}{S_{mn}} = \frac{K_m}{K_n}\,\frac{1-j\,\mathrm{Im}(Z_{rm})/\mathrm{Re}(Z_{rm})}{1-j\,\mathrm{Im}(Z_{rn})/\mathrm{Re}(Z_{rn})}. \quad (20)$$

Another proof of this generalized result is given in [3].

For the conventional S matrix relating the traveling wave amplitudes, $Z_{rn} = Z_{on}$ and (20) becomes

$$\frac{S_{nm}^o}{S_{mn}^o} = \frac{K_m}{K_n}\,\frac{1-j\,\mathrm{Im}(Z_{om})/\mathrm{Re}(Z_{om})}{1-j\,\mathrm{Im}(Z_{on})/\mathrm{Re}(Z_{on})} = \frac{\overline{p_{om}}/\mathrm{Re}(p_{om})}{\overline{p_{on}}/\mathrm{Re}(p_{on})}. \quad (21)$$

The corresponding condition on the impedance parameters Z_{nm}, defined by $v_m = \sum_n Z_{mn}i_n$, is [3]

$$\frac{Z_{nm}}{Z_{mn}} = \frac{K_m}{K_n}\,\frac{v_{on}v_{om}^*}{v_{on}^*v_{om}}. \quad (22)$$

Equations (20), (21), and (22) all involve the reciprocity factors K_n for each guide. While the phase of K_n depends directly on the normalization of $\boldsymbol{e}_n$ and $\boldsymbol{h}_n$, its magnitude is unique, independent of the choice of voltage path in (3) and of the choice of normalization of $\boldsymbol{e}_n$ and $\boldsymbol{h}_n$. The phase of the characteristic impedance is also independent of these normalizations. Thus, the quantities $|S_{mn}^o/S_{mn}^o|$ and $|Z_{nm}/Z_{mn}|$ are unique and independent of normalization as well. Note that the Z_{nm} are defined directly in terms of the waveguide voltages and currents and are independent of the wave definitions and normalizations. Thus, the appearance of the reciprocity factor in (22) most clearly illustrates the fundamental difference between these and previously reported results.

IV. Partially Filled Waveguide

If the phase of the electric field is constant across a waveguide, then the magnitude of the reciprocity factor K for that guide must be 1. Otherwise, such as when the waveguide is partially filled with a lossy dielectric, K may differ from 1.

We calculated the magnitude of the reciprocity factor of the dominant mode of a rectangular waveguide partially filled with a lossy dielectric following Harrington [6] and plotted the reciprocity factor in Fig. 2. The continuity of the normal component of the electric displacement across the air–dielectric boundary forces the electric field to change phase across that boundary. This results in a complex reciprocity factor with magnitude less than 1, as illustrated in Fig. 2. For a junction connecting this waveguide to a hollow rectangular waveguide of the same dimensions, application of (20) and (22) shows that the impedance matrix is asymmetric and that even when all reference impedances are chosen to be real, the forward and reverse transmission coefficients are unequal.

V. Coxial Lines

The phases of the electric and magnetic fields are nearly constant over the cross section of many common guides. Coaxial lines, hollow rectangular and circular waveguide, and, to a lesser extent, quasi-TEM lines are examples. We expect

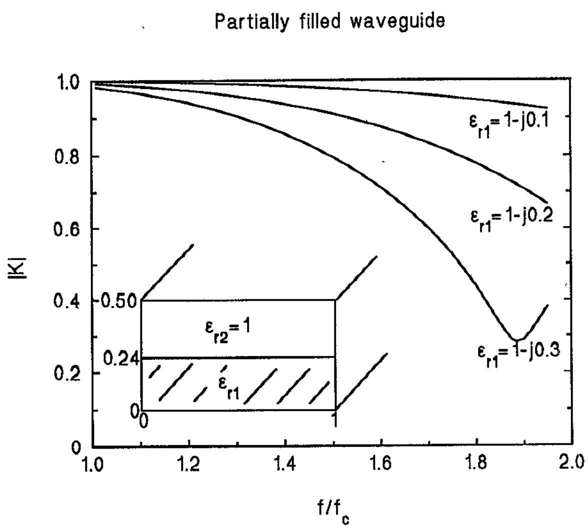

Fig. 2. The magnitude of the reciprocity factor for the dominant mode in a waveguide partially filled with a lossy dielectric. The frequency is normalized to the cutoff frequency of the mode in the empty guide.

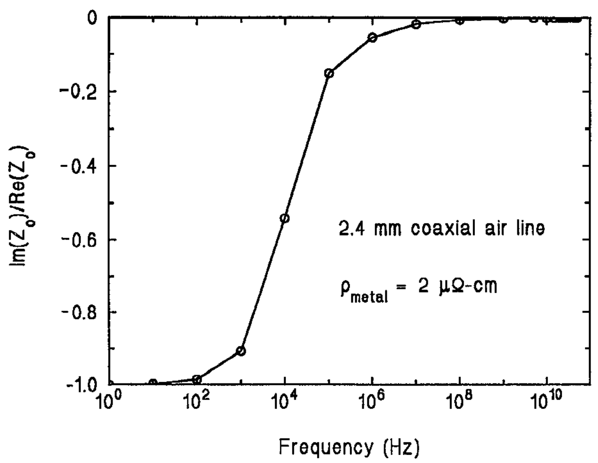

Fig. 3. $\mathrm{Im}(Z_o)/\mathrm{Re}(Z_o)$, equal to the tangent of the phase of Z_o, for a 2.4 mm coaxial line. The center conductor has a diameter of 1.042 mm and metal resistivity of 2 2 $\mu\Omega \cdot$ cm. The plotted values were calculated using the results of Daywitt [7].

the magnitude of the reciprocity factor to be nearly 1 in these guides.

We investigated the reciprocity factor of 2.4 mm coaxial air lines using the calculation technique of Daywitt [7], which rigorously includes the penetration of fields into lossy metal conductors. The phases of the electric and magnetic fields are nearly constant, and the magnitude of K is nearly 1 at low frequencies. Even at 50 GHz, which is near the frequency at which higher-order modes begin to propagate, the magnitude of K deviates from 1 by less than 3×10^{-10}. Thus, in coaxial lines, the impedance matrix is nearly symmetric and the phase of the reference or characteristic impedance is the only significant factor in (20) and (21).

Reference [8] noted that the characteristic impedance of coaxial air lines varies greatly at low frequencies where, in the limit, the phase angle of Z_o approaches $-45°$. Thus, the contribution of the phase of Z_o in (21) cannot be ignored at low frequencies. This is illustrated in Fig. 3.

VI. The Experimental Determination of $|S_{21}/S_{12}|$

The magnitudes of S_{21}^o and S_{12}^o of a waveguide junction may, in principle, be determined directly from microwave power measurements. The procedure begins with the measurement of the power transferred from a source into a power meter, both of which are reflectionless with respect to the traveling waves in the waveguide of port 1 of the junction. Then port 1 of the junction is connected to the source, and port 2 to a second power meter which is reflectionless with respect to the traveling waves in the waveguide of port 2 of the junction. The ratio of the two powers is $|S_{21}^o|^2 \cdot |S_{12}^o|^2$ may also be measured by reversing the experiment. The quotient $|S_{21}^o/S_{12}^o|$ then tests the reciprocity condition. If the experiment is performed on a *reflectionless* junction, and $|S_{21}^o| \neq |S_{12}^o|$, the difference in the measured power ratios is entirely due to the preferential abosrption of power traveling in one of the two directions within the junction. If, instead, the sources and power meters in the experiment are reflectionless with respect to pseudowaves in the two waveguides, the ratio $|S_{21}/S_{12}|$ is determined.

In [9] we reported a similar experiment for a junction connecting a 2.4 mm coaxial line and a coplanar waveguide (CPW) line. The waveguide junction was a microwave probe, and power from a microwave power source was transferred through it to a thermistor bead mounted in a short section of CPW.

In the experiment reported in [9], the product $S_{21}^o S_{12}^o$ was determined by the two-tier TRL de-embedding technique, allowing the ratio $|S_{21}^o/S_{12}^o|$ to be determined without a reverse power measurement. Furthermore, neither the microwave source nor the thermistor bead was reflectionless. To take that into account, the transducer efficiency η of the microwave probe and the short section of CPW line that it contacted, given by

$$\eta \equiv \frac{P_L}{P_A}, \tag{23}$$

was measured. Here P_A is the power available from the source, and P_L is the power delivered to the load. The transducer efficiency η is the equivalent of the transducer power gain described in [10], or the inverse of the transducer loss described in [11]. In the experiment, P_A was determined by first connecting the source to a calibrated coaxial sensor head and measuring the power dissipated in the sensor head. Then the reflection coefficients of the source and sensor head were measured, and P_A calculated form the data. P_L was determined by a dc substitution technique.

The transducer efficiency of the probe (including the short section of CPW line) is related to its pseudoscattering parameters by (24) shown below [9] where Γ_S and Γ_L are the

$$\eta = \frac{|S_{21}|^2\left(1 - |\Gamma_S|^2\right)\left(1 - |\Gamma_L|^2 - 2\,\mathrm{Im}(\Gamma_L)\,\mathrm{Im}(Z_{r2})/\mathrm{Re}(Z_{r2})\right)}{|(1 - S_{11}\Gamma_S)(1 - S_{22}\Gamma_L) - S_{21}S_{12}\Gamma_S\Gamma_L|^2}, \tag{24}$$

$$\left|\frac{S_{21}}{S_{12}}\right| = \frac{\eta|(1 - S_{11}\Gamma_S)(1 - S_{22}\Gamma_L) - S_{21}S_{12}\Gamma_S\Gamma_L|^2}{|S_{21}S_{12}|\left(1 - |\Gamma_S|^2\right)\left(1 - |\Gamma_L|^2 - 2\,\mathrm{Im}(\Gamma_L)\,\mathrm{Im}(Z_{r2})/\mathrm{Re}(Z_{r2})\right)}. \tag{25}$$

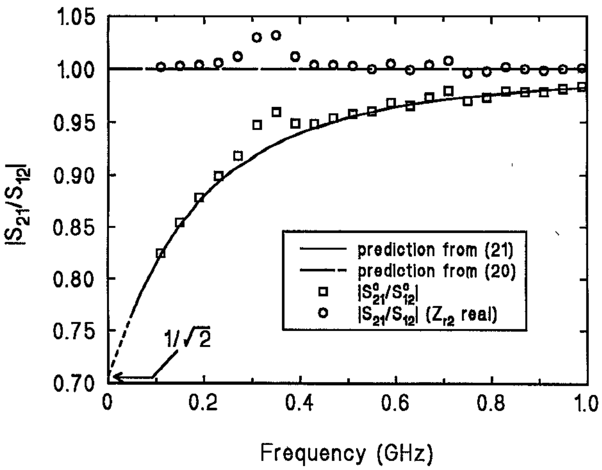

Fig. 4. Measurements of $|S^o_{21}/S^o_{12}|$ and $|S_{21}/S_{12}|$ (with Z_{r2} real) based on (25) compared to the values calculated from (20) and (21) under the assumption $|K_1| = |K_2| = 1$. The calculated and measured results agree closely, and $|S^o_{21}/S^o_{12}|$ deviates significantly from unity, especially at the low frequencies. At very low frequencies, the prediction from (21) approaches $1/\sqrt{2}$ because the phase angles of Z_{o2} approaches $-45°$ [8].

reflection coefficients of the microwave source and thermistor bead, respectively, and Z_{r2} is the reference impedance at the CPW port. Rearrangement of (24) then allows us to write $|S_{21}/S_{12}|$ strictly in terms of measured quantities (25).

In the squares of Fig. 4, we have plotted $|S^o_{21}/S^o_{12}|$, as determined from (25). In the experiment, S^o_{11}, S^o_{22}, and $S^o_{21}S^o_{12}$, the scattering parameters of the intervening probe and line, were measured using the two-tier multiline TRL de-embedding technique [12]. The characteristic impedance Z_{o2} of the CPW was determined from its propagation constant using the technique of [8]. The agreement is good, and $|S^o_{21}/S^o_{12}|$ deviates significantly from 1, especially at the low frequencies. At very low frequencies, the prediction form (21) approaches $1/\sqrt{2}$ because the phase angle of Z_{o2} approaches $-45°$ [8].

For comparison, we have also plotted $|S_{21}/S_{12}|$, represented by circles in the figure, for the case when the calibration reference impedance at the CPW port is set real. The measured data plotted in Fig. 4 are compared to the predictions of (20) and (21) under the assumption that $|K_1| = |K_2| = 1$ (see dashed and solid lines in Fig. 4). Again, the agreement is quite good.

VII. Conclusions

We have derived a general condition relating the forward and reverse transmission coefficients of a reciprocal junction connected to uniform but otherwise arbitrary waveguides. The condition differs from the usual relation equating the two transmission coefficients in that it involves a reciprocity factor and the phase angle of the reference impedance in each guide connected to the junction.

In lossless TEM, TE, and TM guides, the characteristic impedance is real and the reciprocity factor can be chosen to be 1 (see the Appendix). If this is done, the usual relation equating the actual forward and reverse transmission coefficients holds. Some other less common conditions for which this is true are discussed in the Appendix.

In coaxial lines constructed with typically lossy metals, the magnitude of the reciprocity factor is nearly 1, and its deviation from unity can be safely neglected. The phase of the characteristic impedance, however, must be considered at low frequencies. The simplest method of properly accounting for the phase of the characteristic impedance is to use the pseudowaves with a real reference impedance, rather than the traveling waves, in the formulation. Then the forward and reverse transmission parameters of a reciprocal junction are nearly equal.

Our experiments indicate that the reciprocity factor can also be safely neglected in coplanar lines. The experimental evidence showed that at low frequencies, the effects of the complex characteristic impedance, however, are large even at moderately higher frequencies and cannot be neglected.

We also presented an example of a rectangular waveguide partially loaded with a lossy dielectric that showed that the magnitude of the reciprocity factor may deviate significantly from 1. Thus, in some circumstances, both the phase of the characteristic impedance and the magnitude of the reciprocity factor must be considered to determine the relation between the forward and reverse transmission parameters of a reciprocal junction. In this case, even the impedance matrix is asymmetric.

Appendix I
Common Conditions for Which $|K_n| = 1$

The phases of the transverse electric and magnetic fields in lossless guides are constant and equal over the guide cross section. Thus, the characteristic impedance is real and the magnitude of the reciprocity factor is 1 in lossless guides. If, as is conventional, $\boldsymbol{e}_n$ and $\boldsymbol{h}_n$ are chosen to be real, $K_n = 1$.

It is possible to write the reciprocity factor as

$$K_n = \frac{\int_{\sigma_n} \epsilon \boldsymbol{e}_n \cdot \boldsymbol{e}_n \, dS + \int_{\sigma_n} \mu h_{zn}^2 \, dS}{\int_{\sigma_n} \epsilon |\boldsymbol{e}_n|^2 \, dS - \int_{\sigma_n} \mu^* |h_{zn}|^2 \, dS} \tag{26}$$

$$= \frac{\gamma_n^*}{\gamma_n} \frac{\int_{\sigma_n} \mu \boldsymbol{h}_n \cdot \boldsymbol{h}_n \, dS + \int_{\sigma_n} \epsilon e_{zn}^2 \, dS}{- \int_{\sigma_n} \mu^* |\boldsymbol{h}_n|^2 \, dS + \int_{\sigma_n} \epsilon |e_n|^2 \, dS} \tag{27}$$

where γ_n is the propagation constant of the nth mode. Thus, if the mode is TM ($h_{zn} = 0$) and the phase of $\boldsymbol{e}_n$ is constant, then (26) implies $|K_n| = 1$. While TEM guides satisfy these conditions, not all TM guides do. The lossy coaxial lines studied here, for example, are TM but the magnitude of K_n is not exactly equal to 1. If the mode is TE ($e_{zn} = 0$), μ is real, and the phase of $\boldsymbol{h}_n$ is constant, then (27) implies $|K_n| = 1$.

References

[1] R.E. Collin, *Foundations for Microwave Engineering.* New York: McGraw-Hill, 1966, pp. 159–174.
[2] R.F. Bauer and P. Penfield, "De-embedding and unterminating," *IEEE Trans. Microwave Theory Tech.*, vol. MTT-22, pp. 282–288, Mar. 1974.
[3] R.B. Marks and D.F. Williams, "A general waveguide circuit theory," *J. Res. Nat. Inst. Stand. Technol.*, vol. 97, pp. 533–562, Sept.–Oct. 1992.
[4] ——, "Reciprocity relations for on-wafer power measurement," in *38th Automat. RF Tech. Group Conf. Dig.*, San Diego, CA, Dec. 1991, pp. 82–89.
[5] K. Kurokawa, "Power waves and the scattering matrix," *IEEE Trans. Microwave Theory Tech.*, vol. MTT-13, pp. 194–202, 1965.

[6] R. F. Harrington, *Time-Harmonic Electromagnetic Fields.* New York: McGraw-Hill, pp. 158–159, 1961.
[7] W. C. Daywitt, "Exact principal mode field for a lossy coaxial line," *IEEE Trans. Microwave Theory Tech.,* vol. MTT-39, pp. 1313–1322, Aug. 1991.
[8] R. B. Marks and D. F. Williams, "Characteristic impedance determination using propagation constant measurement," *IEEE Microwave Guided Wave Lett.,* vol. 1, pp. 141–143, June 1991.
[9] D. F. Williams and R. B. Marks, "Wafer probe transducer efficiency," *IEEE Microwave Guided Wave Lett.,* vol. 2, pp. 388–390, Oct. 1992.
[10] "S-parameter design," Hewlett Packard Appl. Note 154, p. 23, Apr. 1972 (revised May 1973).
[11] D. M. Kerns and R. W. Beatty, *Basic Theory of Waveguide Junctions and Introductory Microwave Network Analysis.* Oxford: Pergamon Press, 1967, pp. 53–59.
[12] R. B. Marks, "A multi-line method of network analyzer calibration," *IEEE Trans. Microwave Theory Tech.,* vol. MTT-39, pp. 1205–1215, 1991.

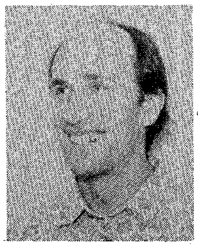

Dylan F. Williams received the Ph.D. degree in electrical engineering from the University of California, Berkeley, in 1986.

In 1986 he joined the Ball Communications Systems Division to work on microwave measurement techniques. In 1989 he joined the Microwave metrology Group at the National Institute of Standards and Technology where he has been studying planar transmission lines and measurements for MMIC's.

Dr. Williams was awarded a Department of Commerce Bronze Medal in 1992 and is a member of Phi Beta Kappa.

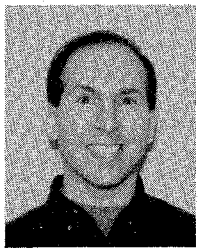

Roger B. Marks received the A.B. degree in physics from Princeton University, Princeton, NJ, in 1980, the M.S. degree in electrical engineering from the University of Utah in 1982, and the Ph.D. degree in applied physics from Yale University, New Haven, CT, in 1988, subsequently serving as a Postdoctoral Research Associate at the Technical University of Delft, The Netherlands.

He has since been with the Electromagnetic Fields Division of the National Institute of Standards and Technology.

Dr. Marks received the Department of Commerce Bronze Medal, in 1992, for his work developing methods for the characterization of monolithic microwave integrated circuits and interconnects.